Biogeosciences, 10, 2001–2010, 2013
www.biogeosciences.net/10/2001/2013/
doi:10.5194/bg-10-2001-2013

Biogeosciences Open Access

Stable isotope and modelling evidence for CO_2 as a driver of glacial–interglacial vegetation shifts in southern Africa

F. J. Bragg[1,2], I. C. Prentice[1,3,4], S. P. Harrison[2,3], G. Eglinton[1,5,6], P. N. Foster[1], F. Rommerskirchen[7,8], and J. Rullkötter[7]

[1]Department of Earth Sciences, University of Bristol, Wills Memorial Building, Bristol BS8 1RJ, UK
[2]School of Geographical Sciences, University of Bristol, Bristol BS8 1SS, UK
[3]Department of Biological Sciences, Macquarie University, North Ryde, NSW 2109, Australia
[4]Grantham Institute for Climate Change and Department of Life Sciences, Imperial College, Silwood Park Campus, Ascot SL5 7PY, UK
[5]Dartmouth College, Hanover, NH 03755, USA
[6]Department of Marine Chemistry and Geochemistry, Woods Hole Oceanographic Institution, 266 Woods Hole Road, Woods Hole, MA 02543-1050, USA
[7]Institute for Chemistry and Biology of the Marine Environment (ICBM), Carl von Ossietzky University of Oldenburg, P.O. Box 2503, 26111 Oldenburg, Germany
[8]MARUM, University of Bremen, Leobener Straße, 28359 Bremen, Germany

Correspondence to: I. C. Prentice (colin.prentice@mq.edu.au)

Received: 19 June 2012 – Published in Biogeosciences Discuss.: 9 November 2012
Revised: 11 February 2013 – Accepted: 4 March 2013 – Published: 22 March 2013

Abstract. Atmospheric CO_2 concentration is hypothesized to influence vegetation distribution via tree–grass competition, with higher CO_2 concentrations favouring trees. The stable carbon isotope ($\delta^{13}C$) signature of vegetation is influenced by the relative importance of C_4 plants (including most tropical grasses) and C_3 plants (including nearly all trees), and the degree of stomatal closure – a response to aridity – in C_3 plants. Compound-specific $\delta^{13}C$ analyses of leaf-wax biomarkers in sediment cores of an offshore South Atlantic transect are used here as a record of vegetation changes in subequatorial Africa. These data suggest a large increase in C_3 relative to C_4 plant dominance after the Last Glacial Maximum. Using a process-based biogeography model that explicitly simulates ^{13}C discrimination, it is shown that precipitation and temperature changes cannot explain the observed shift in $\delta^{13}C$ values. The physiological effect of increasing CO_2 concentration is decisive, altering the C_3/C_4 balance and bringing the simulated and observed $\delta^{13}C$ values into line.

It is concluded that CO_2 concentration itself was a key agent of vegetation change in tropical southern Africa during the last glacial–interglacial transition. Two additional inferences follow. First, long-term variations in terrestrial $\delta^{13}C$ values are not simply a proxy for regional rainfall, as has sometimes been assumed. Although precipitation and temperature changes have had major effects on vegetation in many regions of the world during the period between the Last Glacial Maximum and recent times, CO_2 effects must also be taken into account, especially when reconstructing changes in climate between glacial and interglacial states. Second, rising CO_2 concentration today is likely to be influencing tree–grass competition in a similar way, and thus contributing to the "woody thickening" observed in savannas worldwide. This second inference points to the importance of experiments to determine how vegetation composition in savannas is likely to be influenced by the continuing rise of CO_2 concentration.

1 Introduction

The effects of changes in atmospheric CO_2 concentration on vegetation composition and biome distribution have received relatively little attention, compared with its effects on primary productivity (Ainsworth and Piao, 2005;

Norby et al., 2005) and the terrestrial carbon sink (Prentice et al., 2001; Friedlingstein et al., 2006). Rising CO_2 has however been suggested as one potential cause of "woody thickening". Woody thickening is the widely observed increase of tree and shrub density in savannas (Prentice et al., 2001; Archer et al., 1995, 2001; Bond and Midgely, 2000; MacInnis-Ng et al., 2011). The large (~ 100 ppm) increase in CO_2 concentration over the last glacial–interglacial transition has also been proposed as a major cause of the increase in global forest cover shown by pollen records (Street-Perrott et al., 1997; Jolly and Haxeltine, 1997; Cowling, 1999; Cowling and Sykes, 1999; Bond et al., 2003; Harrison and Prentice, 2003; Cowling and Shin, 2006).

Increasing CO_2 concentration would be expected to favour trees over grasses by increasing the growth rates of trees (C_3) relative to tropical grasses (C_4), which are less responsive to CO_2 (Ehleringer et al., 1997), and more generally by allowing faster-growing tree seedlings to escape the "fire trap" in fire-prone grasslands and savannas (Bond and Midgley, 2000; Bond et al., 2008; Kgope et al., 2010). Global vegetation models predict that increasing CO_2 concentration should generally favour trees, especially but not exclusively in the tropics, both during the transition from the Last Glacial Maximum (LGM) to the Holocene and under present conditions of rising CO_2 (Bond and Midgely, 2000; Bond et al., 2003; Harrison and Prentice, 2003; Prentice and Harrison, 2009; Prentice et al., 2011a). Global modelling has also shown that physiological effects of the change in CO_2 concentration over the last deglaciation must be considered in order to reproduce the increase in forest cover shown by pollen records (Harrison and Prentice, 2003; Prentice and Harrison, 2009).

Pollen analysis provides the most abundant data on past vegetation globally, but pollen records are sparse in the tropics and Southern Hemisphere. An additional, spatially integrated vegetation "sensor" is provided by stable carbon isotope ($\delta^{13}C$) analysis of plant debris and residues (Eglinton and Eglinton, 2008): in particular, compound-specific $\delta^{13}C$ analysis of *n*-alkanes in offshore marine sediments. Long-chain *n*-alkanes are of terrestrial origin (Pearson and Eglinton, 2000). They are deflated and abraded from the waxy cuticles of vascular plants and transported to the marine environment directly and in soil and dust particles by the prevailing winds, and more locally by rivers. The $\delta^{13}C$ values of plant material are strongly dependent on the photosynthetic pathway (Farquhar et al., 1982; Farquhar, 1983). C_4 plants discriminate against ^{13}C by ~ 4 to 8 ‰ and C_3 plants by ~ 14 to 24 ‰. The range of values for C_3 plants reflects the influence of aridity, as discrimination by C_3 photosynthesis is weaker under drier conditions due to stomatal closure (Farquhar et al., 1982; Lloyd and Farquhar, 1994; Diefendorf et al., 2010; Prentice et al., 2011b). The stable carbon isotope signature of cuticular *n*-alkanes reflects that of the total leaf lipids from which they originated, with an average offset of -6 ‰ for C_3 vegetation and -10 ‰ for C_4 vegetation (Collister et al., 1994). To first order, changes in the $\delta^{13}C$ of these biomarkers thus indicate changes in the balance of C_3 and C_4 plants in the source vegetation, with less negative values indicating more C_4 plants. This signal is overprinted by an effect of aridity on C_3 photosynthesis: for a given ratio of C_3 to C_4 foliage biomass, less negative values imply a drier environment.

We used a data set (Rommerskirchen et al., 2003, 2006) of *n*-alkane $\delta^{13}C$ measurements from sediments corresponding to the period around the LGM (Marine Isotope Stage 2, MIS 2) and the Holocene (Marine Isotope Stage 1, MIS 1), taken along a meridional transect of marine cores to the west of subequatorial Africa (Fig. 1). These data have relatively low temporal resolution and thus represent averaged conditions within each period, allowing us to focus on the contrast between them. The data show similar values for $\delta^{13}C$ in MIS 1 and 2 south of about 20° S. Between the equator and 20° S, however, the values for the two periods differ by up to 5 ‰. This difference has been used to suggest a substantially greater vegetation representation of C_4 plants in tropical Africa during MIS 2, which in turn would imply a major expansion of tropical forests at the expense of C_4 grasslands during the transition from the LGM to the Holocene (Rommerskirchen et al., 2006). Additionally, supporting latitudinal $\delta^{13}C$ data on leaf-wax *n*-alkanes in south-eastern Atlantic Ocean sediments have recently been obtained by Vogts (2011) and Vogts et al. (2012), who sampled an isobathic transect of surface sediments from 1° N to 28° S. The n-$C_{29–33}$ weighted-mean $\delta^{13}C$ values increased from -33 ‰ in the north to around -26 ‰ in the south. The latitudinal trend and absolute $\delta^{13}C$ values of the *n*-alkanes along this 13-site transect (~ 1300 m water depth) closely match those of the 9-site Holocene transect (738 to 3973 m water depth) shown in Fig. 1.

We used climate model simulations of LGM and Holocene climates to drive a state-of-the-art biogeography model that explicitly simulates the C_3/C_4 plant balance and ^{13}C discrimination by plants. Our goal was an overall assessment of the importance of changes in climate (including annual and seasonal precipitation and temperature changes) versus physiological CO_2 effects in driving the observed large temporal shift in $\delta^{13}C$ values between glacial and interglacial vegetation in the tropical part of the transect.

2 Methods

We used recent climate data and Palaeoclimate Modelling Intercomparison Project (PMIP) Phase 2 simulations of the global climate (Braconnot et al., 2007) during the mid-Holocene (MH; defined as 6000 yr before present) and the LGM (21 000 yr before present) to drive the state-of-the-art coupled equilibrium biogeochemistry–biogeography model, BIOME4 (Kaplan, 2001; Kaplan et al., 2003). Trajectory analysis was used to estimate probabilities of different contributing source areas for deflated plant material in each

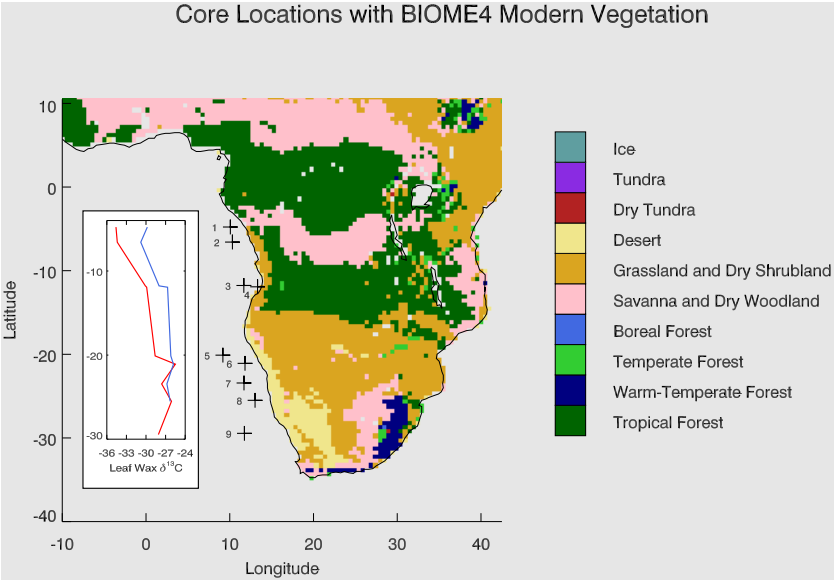

Fig. 1. Locations of the marine core sites, and the δ^{13}C data of leaf-wax *n*-alkanes extracted from Holocene (red) and LGM (blue) sediments as a function of latitude. Data from Rommerskirchen et al. (2003, 2006). Vegetation as modelled by BIOME4.

marine core. Simulated δ^{13}C values at contributing grid cells were then averaged with weighting according to leaf area index (representing the surface area of deflatable material) and estimated source probability.

2.1 Climate model simulations

The PMIP MH climate simulations include the effects of changing orbital parameters, affecting the seasonal and latitudinal distribution of insolation, during the Holocene. They were driven with pre-industrial CO_2 concentration (280 ppm) while methane concentration was reduced, following the PMIP Phase 2 protocol. The PMIP LGM climate simulations include orbital parameters closer to today's, but impose large continental ice sheets specified from ICE5G (Peltier, 2004) and reduced atmospheric concentrations of the three long-lived biogenic greenhouse gases (methane, nitrous oxide and CO_2). LGM climate model simulations, combined with biosphere models, can reproduce the broad-scale global patterns of glacial–interglacial vegetation changes (as shown by pollen data) provided physiological effects of changing CO_2 concentration are taken into account (Harrison and Prentice, 2003; Prentice et al., 2011a). We used the ECHAM, FGOALS, FOAM, IPSL, MIROC, MRI-fa, MRI-nfa and UBRIS model simulations for the MH and the FGOALS, HadCM3, IPSL and MIROC model simulations for the LGM. These were the models whose outputs were available in the PMIP archive (http://pmip2.lsce.ipsl.fr/), and provided all of the model output fields required to drive BIOME4 at the time when the archive was accessed.

2.2 Biogeography model simulations

A single pre-industrial Holocene (PI) vegetation simulation was obtained by driving BIOME4 with contemporary climate but with CO_2 concentration set at the pre-industrial value of 280 ppm. Palaeosimulations with BIOME4 were obtained after adding anomalies (differences between simulated palaeo- and control model runs) of monthly climate variables to the contemporary climate baseline. We generated climate–model anomaly fields for each monthly mean climate variable (12 variables for temperature, 12 for precipitation and 12 for fractional sunshine hours) and interpolated these to the BIOME4 grid. Absolute minimum temperature values, required by BIOME4 to locate the boundary between tropical and non-tropical woody biomes, were adjusted from modern values by finding the coldest month separately for each grid cell in the climate data set and applying the anomaly of the monthly minimum temperature values for that month to the modern absolute minimum temperature. The entire procedure was carried out separately using the output of each climate model. Additional simulations were performed using the averaged outputs of all the MH climate model runs, and all the LGM climate model runs, for the purpose of generating palaeobiome maps.

A CO_2 concentration of 280 ppm was prescribed for all the MH runs of BIOME4 and also for LGM *climate-only* runs to demonstrate the effect of changing to a glacial climate without lowering CO_2. For the *full* LGM runs, a CO_2 concentration of 189 ppm was prescribed. The value of 189 ppm was chosen because it represents the average of ice-core measurements of the CO_2 concentration in MIS 2 (Petit et al., 1999).

2.3 Modelling stable carbon isotope composition

BIOME4 simulates average ^{13}C discrimination by vegetation (Kaplan et al., 2002). The ^{13}C computation is summarized in Appendix A. It accounts both for changes in the balance of C_3 and C_4 plants, which can be influenced by CO_2 concentration, temperature and precipitation, and changes in stomatal conductance related to moisture availability in C_3 plants. Observed large-scale spatial variations in tissue $\delta^{13}C$ at the leaf level, respired CO_2 at the ecosystem level, and latitudinal variations in the $\delta^{13}C$ values of biospheric CO_2 sources and sinks contributing to measured seasonal cycles of $\delta^{13}CO_2$ in the atmosphere can all be well simulated using this scheme (Kaplan et al., 2002).

2.4 Estimating and applying source areas

The prevailing winds today track consistently from east to west across subequatorial Africa. PMIP simulations for subequatorial Africa show only slight changes in wind strength and direction across Africa from LGM to MH and recent times, except in the southernmost part of the continent (Braconnot et al., 2007). We therefore used modern wind trajectory data to approximate the past and present continental source areas of each marine core. Each marine core location was subjected to a back-trajectory wind analysis using the HYSPLIT tool, available at the National Oceanic and Atmospheric Administration's Real-time Environmental Applications and Display sYstem (READY) website (http://www.arl.noaa.gov/ready/hysplit4.html). Altogether, 216 trajectories ($6\,\mathrm{yr} \times 12$ months $\times\, 3$ heights) were obtained for each core location tracking back for 5 days (see Fig. S1 in the Supplement). Probabilities for each 0.5° grid cell in the region considered were obtained as frequencies for each trajectory to pass over the grid cell based on the method of Lunt et al. (2001), then weighted by leaf area index for the cell to account for spatial variations in the amount of leaf material available for deflation.

As a simple alternative and robustness test, we considered latitude bands, 5° wide, extending from the west coast to 30° E, centred on the latitude of each core, with weighting again by leaf area index but with all grid cells in the band considered to have an equal probability of being a source. The results (not shown) were nearly identical.

Isotopic values for each core location, simulated as described above, were converted to represent *n*-alkane values by applying the average offset values from Collister et al. (1994), linearly interpolated between the end-member values for C_3 and C_4 plants according to the relative amounts of modelled C_3 and C_4 vegetation in the grid cells. Background (air) $\delta^{13}C$ values were taken to be -6.52 ‰ in the PI and MH and -6.66 ‰ at the LGM (Indermühle et al., 1998; Smith et al., 1999), a difference with only a very minor impact.

3 Results

The PI simulation shows a north–south profile close to the Holocene observations of *n*-alkane $\delta^{13}C$, with values in the range of -24 to -28 ‰ in the southern part of the transect (Fig. 2a). North of 20° S both the observed and modelled values become progressively more negative with decreasing latitude, reaching -32 to -35 ‰ at 5° S. The MH simulations are close to the PI simulation, indicating that the simulated Holocene vegetation changes in this region were relatively minor compared to those between LGM and Holocene. As the $\delta^{13}C$ measurements represent composite sediment samples from a broad time period within MIS 1, they include material representing MH as well as more recent times. The simulated MH $\delta^{13}C$ values for 5 to 7° S (-32 to -33 ‰) are closer to the observed values than the simulated PI values. The differences are small in any case.

The LGM data occupy a similar range of $\delta^{13}C$ values as the Holocene values in the southern part of the transect. North of 20° S they diverge, becoming more negative but less steeply than in the Holocene, reaching only to -30 ‰ by 5° S (Fig. 2a). In contrast, the simulated LGM values based on climate change alone remain close to the observed *Holocene* – not LGM – values. This finding shows that precipitation and temperature changes alone (including the effects of changes in precipitation, and thus moisture availability, on ^{13}C discrimination by C_3 plants) cannot explain the observed change in ^{13}C discrimination between the LGM and Holocene.

Only when realistic LGM CO_2 concentration is applied in the biome simulation do the simulated tropical values show the observed LGM pattern, reaching a value identical to the observed LGM $\delta^{13}C$ value at 5° S. The disparity is seen most clearly in Fig. 2b, which shows the differences (LGM minus Holocene) in the observed $\delta^{13}C$ values, and the corresponding differences (LGM minus PI) in the simulated $\delta^{13}C$ values. North of 20° S, the differences based on the full LGM simulation (with climate change and realistic CO_2 concentration) remain close to the differences seen in the data. Observed and simulated differences are in the range 3.5 ± 1.5 ‰. The differences based on the climate-only LGM simulation are in the range of 0 ± 1 ‰ only, and do not overlap at all with the observed range of differences.

A similar contrast can be seen in the simulated biome distributions (Fig. 3). The LGM climate-only simulation shows a slight *expansion* of tropical forests whereas the full LGM simulation with realistic CO_2 concentration shows a substantial contraction of forests, with grasslands and dry shrublands expanding to largely replace both savanna and forests north of 20° S. The available pollen data for comparison with these simulations (Jolly et al., 1998; Elenga et al., 2000; summarized in Fig. S2 in the Supplement) are too sparse to allow a definitive comparison. They do nonetheless show a contraction of tropical forests at the LGM (Prentice et al., 2000),

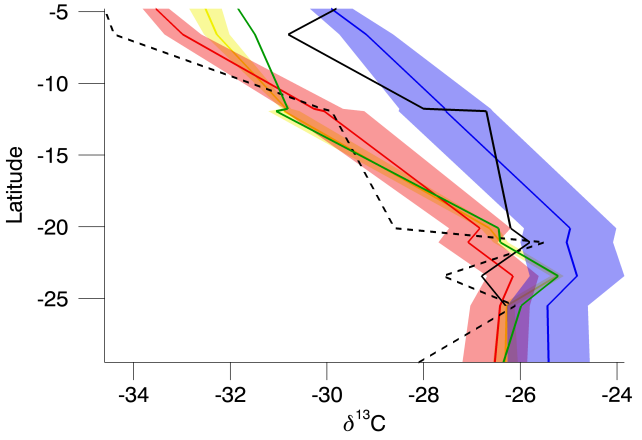

Fig. 2a. (a) Observed and simulated $\delta^{13}C$ values of leaf-wax *n*-alkanes at the core sites as a function of latitude. Dashed black line: holocene data; solid black line: LGM data. Simulations: PI (green), MH (yellow), LGM with pre-industrial CO_2 (280 ppm, red), and LGM with realistic CO_2 (189 ppm, blue).

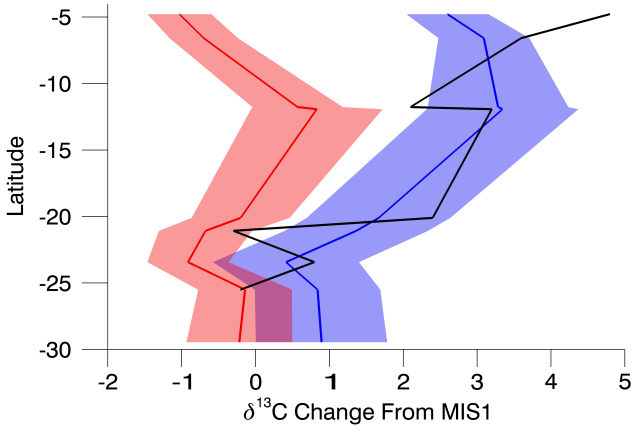

Fig. 2b. (b) Observed and simulated differences in $\delta^{13}C$ values of leaf-wax *n*-alkanes. Black line: data, LGM minus Holocene. Simulations: LGM with pre-industrial CO_2 minus PI (red); LGM with realistic CO_2 minus PI (blue). In both panels, simulated values are shown as means (coloured lines) and ranges (shading) across climate models.

consistent with our full LGM simulations with the CO_2 effect included.

4 Discussion

These results show that the glacial–interglacial climate change, as simulated by the range of PMIP models, qualitatively cannot account for observed stable carbon isotope and vegetation changes in tropical southern Africa. The models show reduced precipitation at the LGM, which is consistent with previous analyses (Gasse, 2000). But the effects of reduced precipitation are by no means large enough to explain the $\delta^{13}C$ measurements. This lack of a strong effect of reduced precipitation can be explained as a consequence of countervailing effects of lower temperatures in reducing evapotranspiration (conserving soil moisture) and photorespiration (allowing greater C_3 plant productivity than would otherwise be possible at low CO_2 concentration) (Cowling and Shin, 2006). On the other hand, the effects of CO_2 concentration as modelled by BIOME4, in combination with the climate change effects, are consistent with the $\delta^{13}C$ data. The modelled effect of CO_2 concentration is a consequence of the strong dependence of C_3 photosynthesis on CO_2 concentration in the subambient range (Polley et al., 1993; Cowling and Sage, 1998; Harrison and Bartlein, 2011), contrasting with the relatively weak effect of CO_2 concentration on plants with C_4 photosynthesis. Our finding points to a key role of atmospheric CO_2 concentration in determining glacial–interglacial biome shifts in this tropical region.

There are implications for the interpretation of palaeo-$\delta^{13}C$ measurements. *n*-alkane $\delta^{13}C$ data from another African margin transect that crosses the equator, extending between 20° N and 20° S, have been interpreted in terms of precipitation change only (Collins et al., 2011). The similarity of observed LGM-to-Holocene $\delta^{13}C$ shifts in the Northern and Southern hemispheres was interpreted as evidence for symmetrical changes in the distribution of rainfall around the equator (Collins et al., 2011). But the long-standing evidence for CO_2 concentration effects on the balance of C_3 trees and C_4 grasses (Bond and Midgley, 2000) contradicts the explicit assumption in Collins et al. (2011) that this balance is controlled only by hydrology. Sinninghe Damsté et al. (2011) presented *n*-alkane $\delta^{13}C$ values from an East African lake core, with much higher temporal resolution than can normally be achieved with marine sediments, and concluded that "rainfall variation by itself is not the single most important driver of long-term vegetation change in this region of tropical Africa…the relatively invariant C_3/C_4 ratio during the glacial and Holocene periods resembles the main long-term trend in atmospheric pCO_2, suggesting substantial control" (Sinninghe Damsté et al., 2011, p. 244). With knowledge of CO_2 effects, apparently symmetrical "expansion of the African rainbelt" from glacial to Holocene periods (Collins et al., 2011) could simply be a consequence of forcing by changes in atmospheric CO_2 concentration. This is bound to be symmetrical because the effects are global, evoking similar responses in the Northern and Southern hemispheres.

There is abundant evidence for regional changes in precipitation and temperature during the period between the LGM and PI, and effects of these changes on vegetation. For example, there were large changes in the Northern Hemisphere monsoons (especially the African monsoon) from the LGM to MH (expansion) and MH to PI (contraction), and associated changes in vegetation cover and hydrology (e.g. Kutzbach and Street-Perrott, 1985; Jolly et al., 1998; Elenga et al., 2000; Gasse, 2000; Prentice et al., 2000). The broad

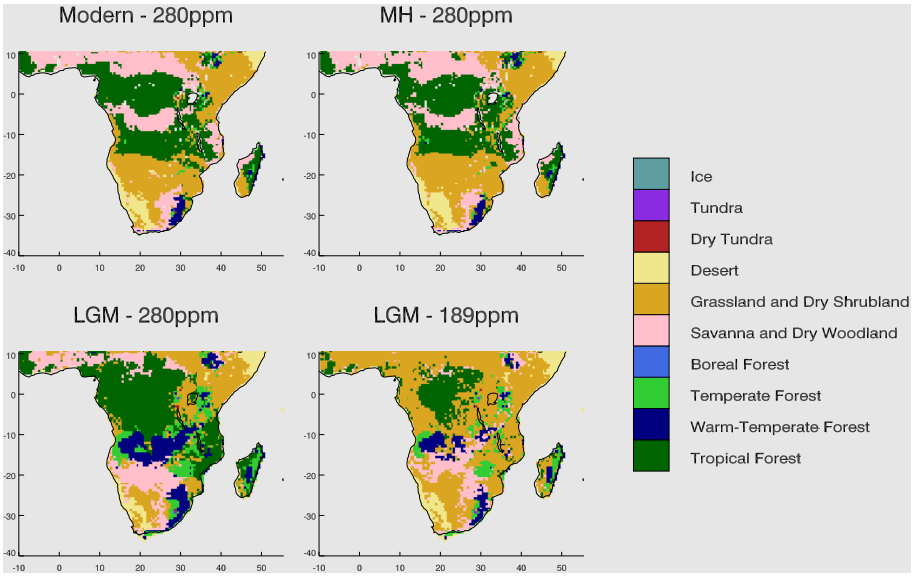

Fig. 3 . Simulated biome distributions for PI, MH (model-average climate), LGM (model-average climate and pre-industrial CO_2, 280 ppm) and LGM (model-average climate and realistic CO_2, 189 ppm).

features of these climate changes can be reproduced by climate models (e.g. COHMAP Members, 1988; Otto-Bliesner et al., 2006; Braconnot et al., 2007), and their effects on vegetation can be modelled as well (e.g. Kutzbach et al., 1998; Kohfeld and Harrison, 2000; Kageyama et al., 2012). Large vegetation changes occurred during the Younger Dryas cold interval (e.g. Sinninghe Damsté et al., 2011), which interrupted the deglacial warming trend even as CO_2 continued to increase, and during the rapid Dansgaard–Oeschger climate changes that punctuated the last glaciation (Harrison and Sanchez-Goñi, 2010). It may be possible to exploit the partial decoupling between CO_2 concentration and climate evident in high-resolution palaeorecords to quantify the relative contributions of CO_2 and climate changes empirically for different periods and regions. This is beyond the scope of the present study where our focus is on the comparison of two broad time periods differing in both CO_2 concentration and climate. Our results nonetheless imply that large CO_2 concentration changes can have major effects on vegetation that should not be ignored when palaeoecological data are used to reconstruct changes in climate (Prentice and Harrison, 2009). CO_2 and climate are combined drivers of vegetation change, not alternatives. The ways in which they combine are relatively well understood (Collatz et al., 1998), and are incorporated in state-of-the-art vegetation models.

This point has sometimes been misunderstood in the Quaternary science literature. For example, Huang et al. (2001) has often been cited as evidence against a CO_2 effect on vegetation changes between the LGM and Holocene. Huang et al. (2001) contrasted a record from tropical Central America with one from south-western North America, a now-arid region that was wet during the LGM, as shown by the former presence of extensive woodlands (Thompson and Anderson, 2000) and vast palaeolakes. The tropical record showed C_4 dominance during the LGM giving way to C_3 dominance during the Holocene, as in this study. The other record showed the opposite trend. But a very wet LGM in that region is consistently predicted by climate models as the result of a circulation shift, forced by the existence of the Laurentide ice sheet (COHMAP Members, 1988; Kutzbach et al., 1998). A shift from C_3 vegetation at LGM to C_4 in the Holocene is modelled for this region (Prentice et al., 2011a) as a consequence of increasing aridity after the LGM. This example demonstrates that our modelling approach can correctly predict situations where effects of changing climate override those of CO_2.

Finally, our results have implications for the interpretation of the trend towards increased tree density in savannas, known as "woody thickening". The effect of CO_2 concentration on photosynthesis in C_3 plants, including trees, is steeper in the lower range than in the present range, but it is still substantial (Cowling and Sage, 1998). By a conservative calculation, assuming a ratio of internal leaf to ambient CO_2 concentration of 0.7, and co-limitation of C_3 photosynthesis by Rubisco and electron transport, an increase of CO_2 concentration from 280 ppm to 380 ppm should have increased the potential growth rates of C_3 plants during the industrial era by $\sim$15 to 20 %. A continued increase from 380 ppm to 550 ppm should cause a further increase of similar magnitude in the potential growth rates of C_3 plants. Given the weak response of C_4 photosynthesis (as used by tropical grasses) to CO_2 concentration, this increase in C_3 photosynthesis would be expected to increase the competitive ability of C_3 plants and thereby influence the balance of C_3 and C_4

plant dominance. The effect should be noticeable even if the CO_2 effect is partially counteracted by other constraints, such as nitrogen limitation and the associated diversion of primary production to root growth (Palmroth et al., 2006; Finzi et al., 2007). In dry environments the effect of rising CO_2 concentration is likely to be greater than this simple calculation suggests, because stomata are more closed (conserving water) in dry environments and so a change in CO_2 has a proportionally larger effect. Our findings do not rule out a contribution to contemporary woody thickening from other factors including land-use change (Archer et al., 1995), but they indicate that continued rise in CO_2 concentration is nonetheless likely to further increase woody plant cover today, just as it did during the worldwide reforestation after the LGM. And whereas the transition from LGM to Holocene has to be understood through reconstruction and modelling, the specific effects of changes from present CO_2 levels are amenable to experiments – not only FACE experiments, which are expensive, but also experiments that could be conducted on a more modest scale to analyse the responses of ecosystems in controlled environments.

Appendix A

Isotopic discrimination in the BIOME4 model

BIOME4 (Kaplan, 2001, Kaplan et al., 2003) is an equilibrium model for large-scale biome distribution based on the comparison of potential net primary production (NPP) for plant functional types (PFTs) that differ in stature, phenology, physiology and bioclimatic requirements. NPP is modelled as a balance of photosynthesis and respiration, allowing the computation of ancillary properties, such as the leaf internal CO_2 concentration (c_i), needed to quantify the discrimination against ^{13}C during photosynthesis (Kaplan et al., 2002). The set of 12 PFTs considered includes various types of (C_3) trees, and both C_4 and C_3 herbaceous plants. Bioclimatic limits provide a coarse environmental filter so that, for example, tropical trees are confined to frost-free climates. Among PFTs allowed by the filter, by default the dominant PFT is chosen to be the tree type with the highest NPP. However, under dry conditions (below an empirically determined threshold value of soil moisture content) herbaceous PFTs are allowed to "compete" with trees; the dominant PFT is then simply the one with the highest NPP. The $\delta^{13}C$ value output by the model applies to the dominant PFT in forests, but is a flux-weighted average of values for the woody and herbaceous PFTs present in mixtures.

Among C_3 plants, each PFT is assigned a maximum value of the ratio c_i/c_a, where c_a is ambient CO_2 concentration. These maximum values were determined by a literature review. The rate of transpiration (E) is the lesser of an evaporative demand term (D) and a supply term (S). The supply term is related to soil moisture, which, in turn, is calculated from the balance of precipitation and evapotranspiration, so precipitation changes affect the c_i/c_a ratio of C_3 plants by way of their effect on this balance. The maximum c_i/c_a ratios apply only so long as $E = D$:

$$D = \alpha_m E_q [1 - \exp(g_p/g_o)], \tag{A1}$$

where $\alpha_m = 1.4$, E_q is the equilibrium rate of evapotranspiration (a function of net radiation and temperature only), g_p is "potential" stomatal conductance (i.e. the value that yields the maximum c_i/c_a ratio), and g_o is a scaling parameter. c_i/c_a ratios are reduced when $S < D$ and thus $E = S$:

$$S = w \cdot E_m, \tag{A2}$$

where w ($0 \le w \le 1$) is relative volumetric soil moisture (a weighted average of the two soil layers, with weighting determined by the specified vertical root profile for the PFT), and E_m is a PFT-specific maximum transpiration rate. Under these conditions, stomatal conductance g_s is determined by the general case of Eq. (1):

$$E = \alpha_m E_q [1 - \exp(g_s/g_o)], \tag{A3}$$

where E is now determined from Eq. (2), yielding

$$g_s = g_o \ln[1/(1 - \alpha^*)], \tag{A4}$$

where

$$\alpha^* = E/\alpha_m E_q. \tag{A5}$$

c_i is then calculated by simultaneous solution of the biochemical and diffusion equations for photosynthesis. Discrimination against ^{13}C is calculated from c_i/c_a following Lloyd and Farquhar (1994):

$$\Delta = 1.9 - 8\Gamma^*/c_a + 23.1 c_i/c_a, \tag{A6}$$

with $\Gamma^* = 1.54\ T$, where T is an estimate of daytime leaf temperature in °C.

Ecosystem Δ values are averages over PFTs, weighted by the gross primary production of each PFT. Discrimination by C_4 photosynthesis is always less than discrimination by C_3 photosynthesis, and is only weakly sensitive to environment. Kaplan et al. (2002) showed that this scheme gives good representations of the large-scale patterns of observed $\delta^{13}C$ values at the level of individual leaf samples, at the ecosystem level based on measurements of respired CO_2, and at the regional level based on "Keeling plots" of $\delta^{13}CO_2$ versus $1/[CO_2]$.

Supplementary material related to this article is available online at: http://www.biogeosciences.net/10/2001/2013/bg-10-2001-2013-supplement.zip.

Acknowledgements. We acknowledge the international modelling groups for providing their data for analysis and the Laboratoire des Sciences du Climat et de l'Environnement (LSCE) for collecting and archiving the model outputs. The PMIP2/MOTIF Data Archive has been supported by CEA, CNRS, the EU project MOTIF (EVK2-CT-2002-00153) and the Programme National d'Etude de la Dynamique du Climat (PNEDC). More information about the PMIP archive is available at http://pmip2.lsce.ipsl.fr/.

Edited by: P. Stoy

References

Ainsworth, E. A. and Piao, S. L.: What have we learned from 15 years of free-air CO_2 enrichment (FACE)? A meta-analytic review of the responses of photosynthesis, canopy properties and plant production to rising CO_2, New Phytol., 165, 351–372, 2005.

Archer, S., Boutton, T. W., and Hibbard, K. A.: Trees in grasslands: biogeochemical consequences of woody plant expansion, in: Global Biogeochemical Cycles in the Climate System, edited by: Schulze, E.-D., Heimann, M., Harrison, S. P., Holland, E. A., Lloyd, J., Prentice, I. C., and Schimel, D. S., Academic Press, San Diego, 115–137, 2001.

Archer, S., Schimel, D. S., and Holland, E. A.: Mechanisms of shrubland expansion: land use, climate or CO_2?, Climatic Change, 29, 91–99, 1995.

Bond, W. J.: What limits trees in C_4 grasslands and savannas?, Annu. Rev. Ecol. Evol. S., 39, 641–659, 2008.

Bond, W. J. and Midgley, G. F.: A proposed CO_2-controlled mechanism of woody plant invasion in grasslands and savannas, Global Change Biol. 6, 865–869, 2000.

Bond, W. J., Midgley, G. F., and Woodward, F. I.: The importance of low atmospheric CO_2 and fire in promoting the spread of grasslands and savannas, Global Change Biol., 9, 973–982, 2003.

Braconnot, P., Otto-Bliesner, B., Harrison, S., Joussaume, S., Peterchmitt, J.-Y., Abe-Ouchi, A., Crucifix, M., Driesschaert, E., Fichefet, Th., Hewitt, C. D., Kageyama, M., Kitoh, A., Laîné, A., Loutre, M.-F., Marti, O., Merkel, U., Ramstein, G., Valdes, P., Weber, S. L., Yu, Y., and Zhao, Y.: Results of PMIP2 coupled simulations of the Mid-Holocene and Last Glacial Maximum – Part 1: experiments and large-scale features, Clim. Past, 3, 261–277, doi:10.5194/cp-3-261-2007, 2007.

COHMAP Members: Climatic changes of the last 18,000 years: observations and model simulations, Science, 241, 1043–1052, 1988.

Collatz, G. J., Berry, J. A., and Clark, J. S.: Effects of climate and atmospheric CO_2 partial pressure on the global distribution of C_4 grasses: present, past, and future, Oecologia, 114, 441–454, 1998.

Collins, J. A., Schefuß, E., Heslop, D., Mulitza, S., Prange, M., Zabel, M., Tjallingii, R., Dokken, T. M., Huang, E., Mackensen, A., Schulz, M., Tian, J., Zarriess, M., and Wefer, G.: Interhemispheric symmetry of the tropical African rainbelt over the past 23,000 years, Nat. Geosci., 4, 42–45, 2011.

Collister, J. W., Rieley, G., Stern, B., Eglinton, G., and Fry, B.: Compound-specific $\delta^{13}C$ analyses of leaf lipids from plants with differing carbon dioxide metabolisms, Org. Geochem. 21, 619–627, 1994.

Cowling, S. A.: Simulated effects of low atmospheric CO_2 on structure and composition of North American vegetation at the Last Glacial Maximum, Global Ecol. Biogeogr., 8, 81–93, 1999.

Cowling, S. A. and Sage, R. F.: Interactive effects of low atmospheric CO_2 and elevated temperature on growth, photosynthesis and respiration in Phaseolus vulgaris, Plant Cell Environ., 21, 427–435, 1998.

Cowling, S. A. and Shin, Y.: Simulated ecosystem threshold responses to co-varying temperature, precipitation and atmospheric CO_2 within a region of Amazonia, Global Ecol. Biogeogr., 15, 553–566, 2006.

Cowling, S. A. and Sykes, M. T.: Physiological significance of low atmospheric CO_2 for plant climate interactions, Quaternary Res., 52, 237–242, 1999.

Diefendorf, A. F., Mueller, K. E., Wing, S. L., Koch, P. L., and Freeman, K. H.: Global patterns in leaf ^{13}C discrimination and implications for studies of past and future climate, P. Natl. Acad. Sci. USA, 107, 5738–5743, 2010.

Eglinton, T. I. and Eglinton, G.: Molecular proxies for paleoclimatology. Earth Planet. Sci. Lett., 275, 1–16, 2008.

Ehleringer, J. R., Cerling, T. E., and Helliker, B. R.: C_4 photosynthesis, atmospheric CO_2 and climate, Oecologia, 112, 285–299, 1997.

Elenga, H., Peyron, O., Bonnefille, R., Jolly, D., Cheddadi, R., Guiot, J., Andrieu, V., Bottema, S., Buchet, G., de Beaulieu, J.-L., Hamilton, A. C., Maley, J., Marchant, R., Perez-Obiol, R., Reille, M., Riollet, G., Scott, L., Straka, H., Taylor, D., Van Campo, E., Vincens, A., Laarif, F., and Jonson, H.: Pollen-based biome reconstruction for southern Europe and Africa 18,000 yr BP, J. Biogeogr., 27, 621–634, 2000.

Farquhar, G. D.: On the nature of carbon isotope discrimination in C_4 species, Aust. J. Plant Physiol., 10, 205–226, 1983.

Farquhar, G. D., O'Leary, M. H., and Berry, J. A.: On the relationship between carbon isotope discrimination and the intercellular carbon dioxide concentration in leaves, Aust. J. Plant Physiol., 9, 121–137, 1982.

Finzi, A. C., Norby, R. J., Calfapietra, C., Gallet-Budynek, A., Gielen, B., Holmes, W. E., Hoosbeek, M. R., Iversen, C. M., Jackson, 5 R. B., Kubiske, M. E., Ledford, J., Liberloo, M., Oren, R., Polle, A., Pritchard, S., Zak, D. R., Schlesinger, W. H., and Ceulemans, R.: Increases in nitrogen uptake rather than nitrogen-use efficiency support higher rates of temperate forest productivity under elevated CO_2, P. Natl. Acad. Sci. USA, 104, 14014–14019, 2007.

Friedlingstein, P., Cox, P., Betts, R., Bopp, L., von Bloh, W., Brovkin, V., Cadule, P., Doney, S., Eby, M., Fung, I., Bala, G., John, J., Jones, C., Joos, F., Kato, T., Kawamiya, M., Knorr, W., Lindsay, K., Mattews, H. D., Raddatz, T., Rayner, P., Reick, C., Roeckner, E., Schnitzler, K.-G., Schnur, R., Strassmann, K., Weaver, A. J., Yoshikawa, C., and Zeng, N.: Climate-carbon cycle feedback analysis: Results from the C4MIP model intercomparison, J. Climate, 19, 3337–3353, 2006.

Gasse, F.: Hydrological changes in the African tropics since the last glacial maximum, Quaternary Sci. Rev., 24, 869–896, 2000.

Harrison, S. P. and Bartlein, P. J.: Records from the past, lessons for the future: what the palaeorecord implies about mechanisms of global change, in: The Future of the World's Climate, edited by: Henderson-Sellers, A. and McGuffi, E. K., Elsevier, 1103, 2011.

Harrison, S. P. and Prentice, I. C.: Climate and CO_2 controls on global vegetation distribution at the last glacial maximum: analysis based on palaeovegetation data, biome modelling and palaeoclimate simulations, Global Change Biol., 9, 983–1004, 2003.

Harrison, S. P. and Sanchez Goñi, M. F. Global patterns of vegetation response to millennial-scale variability and rapid climate change during the last glacial period, Quaternary Sci. Rev., 29, 2957–2980, 2010.

Huang, Y., Street-Perrott, F. A., Metcalfe, S. E., Brenner, M., Moreland, M., and Freeman, K. H.: Climate change as the dominant control on glacial-interglacial variations in C_3 and C_4 plant abundance, Science, 293, 1647–1651, 2001.

Indermühle, A., Stocker, T. F., Joos, F., Fischer, H., Smith, H. J., Wahlen, M., Deck, B., Mastroianni, D., Tschumi, J., Blunier, T., Meyer, R., and Stauffer, B.: Holocene carbon-cycle dynamics based on CO_2 trapped in ice at Taylor Dome, Antarctica, Nature, 398, 121–126, 1998.

Jolly, D. and Haxeltine, A.: Effect of low glacial atmospheric CO_2 on tropical African montane vegetation, Science, 276, 786–788, 1997.

Jolly, D., Prentice, I. C., Bonnefille, R., Ballouche, A., Bengo, M., Brenac, P., Buchet, G., Burney, D., Cazet, J.-P., Cheddadi, R., Edorh, T., Elenga, H., Elmoutaki, S., Guiot, J., Laarif, F., Lamb, H., Lezine, A.-M., Maley, J., Mbenza, M., Peyron, O., Reille, M., Reynaud-Farrera, I., Riollet, G., Ritchie, J. C., Roche, E., Scott, L., Ssemmanda, I., Straka, H., Umer, M., Van Campo, E., Vilimumbalo, S., Vincens, A., and Waller, M.: Biome reconstruction from pollen and plant macrofossil data for Africa and the Arabian peninsula at 0 and 6000 years, J. Biogeogr., 25, 1007–1027, 1998.

Kageyama, M., Braconnot, P., Bopp, L., Mariotti, V., Roy, T., Woillez, M.-N., Caubel, A., Foujols, M. A., Guilyardi, E., Khodri, M., Lloyd, J., Lombard, F., and Marti, O.: Mid-Holocene and last glacial maximum climate simulations with the IPSL model: part II: model-data comparisons, Clim. Dynam., doi:10.1007/s00382-012-1499-5, 2012.

Kaplan, J. O.: Geophysical applications of vegetation modeling, Ph.D. thesis, Lund University, 2001.

Kaplan, J. O., Prentice, I. C., and Buchmann, N., The stable carbon isotope composition of the terrestrial biosphere: modelling at scales from the leaf to the globe, Global Biogeochem. Cy. 16, GB1060, doi:10.1029/2001GB001403, 2002.

Kaplan, J. O., Bigelow, N. H., Prentice, I. C., Harrison, S. P., Bartlein, P. J., Christensen, T. R., Cramer, W., Matveyeva, N. V., McGuire, A. D., Murray, D. F., Razzhivin, V. Y., Smith, B., Walker, D. A., Anderson, P. M., Andreev, A. A., Brubaker, L. B., Edwards, M. E., and Lozhkin, A. V.: Climate change and Arctic ecosystems II: Modeling, paleodata-model comparisons and future projections, J. Geophys. Res., 108, 8171, doi:10.1029/2002JD002559, 2003.

Kgope, B. S., Bond, W. J., and Midgley, G. F.: Growth responses of African savanna trees implicate atmospheric [CO_2] as a driver of past and current changes in savanna tree cover, Austral. Ecol., 35, 451–463, 2010.

Kohfeld, K. E. and Harrison, S. P., How well can we simulate past climates? Evaluating the models using global palaeoenvironmental datasets, Quaternary Sci. Rev., 19, 321–346, 2000.

Kutzbach, J. E. and Street-Perrott, F. A.: Milankovitch forcing of fluctuations in the level of tropical lakes from 18 to 0 kyr BP, Nature, 317, 130–134, 1985.

Kutzbach, J. E., Gallimore, R., Harrison, S. P., Behling, P., Selin, R., and Laarif, F.: Climate and biome simulations for the past 21,000 years, Quaternary Sci. Rev., 17, 473–506, 1998.

Lloyd, J. J. and Farquhar, G. D.: ^{13}C discrimination during CO_2 assimilation by the terrestrial biosphere, Oecologia, 99, 201–215, 1994.

Lunt, D. J. and Valdes, P. J.: Dust transport to Dome C, Antarctica, at the Last Glacial Maximum and present day, Geophys. Res. Lett., 28, 295–298, 2001.

Macinnis-Ng, C., Zeppel, M., Williams, M., and Eamus, D.: Applying a SPA model to examine the impact of climate change on GPP of open woodlands and the potential for woody thickening, Ecohydrology, 4, 379–393, 2011.

Norby, R. J., DeLucia, E. H., Gielen, B., Calfapietra, C., Giardina, C. P., King, J. S., Ledford, J., McCarthy, H. R., Moore, D. J. P., Ceulemans, R., De Angelis, P., Finzi, A. C., Karnosky, D. F., Kubiske, M. E., Lukac, M., Pregitzer, K. S., Scarascia-Mugnozza, G. E., Schlesinger, W. H., and Oren, R.: Forest response to elevated CO_2 is conserved across a broad range of productivity, P. Natl. Acad. Sci. USA, 102, 18052–18056, 2005.

Otto-Bliesner, B. L., Brady, E. C., Clauzet, G., Tomas, R., Levius, S., and Kothvala, Z.: Last glacial maximum and Holocene climate in CCSM3, J. Climate, 19, 2526–2544, 2006.

Palmroth, S., Oren, R., McCarthy, H. R., Johnsen, K. H., Finzi, A. C., Butnor, J. R., Ryan, M. G., and Schlesinger, W. H.: Aboveground sink strength in forests controls the allocation of carbon below ground and its [CO_2]-induced enhancement, P. Natl. Acad. Sci. USA, 103, 19362–19367, 2006.

Pearson, A. and Eglinton, T. I.: The origin of n-alkanes in Santa Monica Basin surface sediment: a model based on compound-specific $\Delta^{14}C$ and $\delta^{13}C$ data, Org. Geochem., 31, 1103–1116, 2000.

Peltier, W. R.: Global glacial isostasy and the surface of the ice-age Earth: the ICE-5G (VM2) model and GRACE, Annu. Rev. Earth Pl. Sc., 32, 111–149, 2004.

Petit, J. R., Jouzel, J., Raynaud, D., Barkov, N. I., Barnola, J.-M., Basile, I., Bender, M., Chappellaz, J., Davis, M., Delaygue, G., Delmotte, M., Kotlyakov, V. M., Legrand, M., Lipenkov, V. Y., Lorius, C., 5 Pépin, L., Ritz, C., Saltzman, E., and Stievenard, M.: Climate and atmospheric history of the past 420,000 years from the Vostok ice core, Antarctica, Nature, 399, 429–436, 1999.

Polley, H. W., Johnson, H. B., Marino, B. D., and Mayeux, H. S.: Increases in C_3 plant water use efficiency and biomass over Glacial to present CO_2 concentrations, Nature, 361, 61–64, 1993.

Prentice, I. C. and Harrison, S. P.: Ecosystem effects of CO_2 concentration: evidence from past climates, Clim. Past, 5, 297–307, doi:10.5194/cp-5-297-2009, 2009.

Prentice, I. C., Jolly, D., and BIOME 6000 participants: Mid-Holocene and glacial-maximum vegetation geography of the northern continents and Africa, J. Biogeogr., 27, 507–519, 2000.

Prentice, I. C., Farquhar, G. D., Fasham, M. J. R., Goulden, M. L., Heimann, M., Jaramillo, V. J., Kheshgi, H. S., Le Quéré, C., Scholes, R. J., and Wallace, D. W. R.: The carbon cycle and atmospheric carbon dioxide, in: Climate Change 2001: The Scientific Basis, edited by: Houghton, J. T., Ding, Y., Griggs, D. J., Noquer, M., van der Linden, P. J., Dai, X., Maskell, K., and Johnson, C. A., Cambridge University Press, Cambridge, UK, 183–224,

2001.

Prentice, I. C., Harrison, S. P., and Bartlein, P. J.: Global vegetation and terrestrial carbon cycle changes after the last ice age, New Phytol., 189, 988–998, 2011a.

Prentice, I. C., Meng, T., Wang, H., Harrison, S. P., Ni, J., and Wang, G.: Evidence of a universal scaling relationship for leaf CO_2 drawdown along an aridity gradient, New Phytol., 190, 169–180, 2011b.

Rommerskirchen, F., Eglinton, G., Dupont, L., Güntner, U., Wenzel, C., and Rullkötter, J.: A north to south transect of Holocene southeast Atlantic continental margin sediments: Relationship between aerosol transport and compound-specific δ^{13}C land plant biomarker and pollen records, Geochem. Geophy. Geosy., 4, 1101, doi:10.1029/2003GC000541, 2003.

Rommerskirchen, F., Eglinton, G., Dupont, L., and Rullkötter, J.: Glacial/interglacial changes in southern Africa: Compound-specific δ^{13}C land plant biomarker and pollen records from southeast Atlantic continental margin sediments, Geochem. Geophy. Geosy., 7, Q08010, 2006.

Sinninghe Damsté, J. S., Verschuren, D., Ossebaar, J., Blokker, J., van Houten, R., Plessen, B., and Schouten, S.: A 25,000-year record of climate-induced changes in lowland vegetation of eastern equatorial Africa revealed by the stable carbon-isotopic composition of fossil plant leaf waxes, Earth Planet. Sci. Lett., 302, 236–246, 2011.

Smith, H. J., Fischer, H., Wahlen, M., Mastroianni, D., and Deck, B.: Dual modes of the carbon cycle since the Last Glacial Maximum, Nature, 400, 248–250, 1999.

Street-Perrott, F. A., Huang, Y., Perrott, R. A., Eglinton, G., Barker, P., Khelifa, L. B., Harkness, D. D., and Olago, D. O.: Impact of lower atmospheric carbon dioxide on tropical mountain ecosystems, Science, 278, 1422–1426, 1997.

Thompson, R. S. and Anderson, K. H.: Biomes of western North America at 18,000, 6000 and 0 ^{14}C yr BP reconstructed from pollen and packrat midden data, J. Biogeogr., 27, 555-584, 2000.

Vogts, A.: Plant wax alkanes and alkan-1-ols in ocean sediments as indicators of continental climate change – validation of a molecular proxy, Ph.D. thesis, University of Oldenburg, Germany, available at: http://oops.uni-oldenburg.de/volltexte/2011/1192, 2011.

Vogts, A., Schefuß, E., Badewien, T., and Rullkötter, J.: *n*-Alkane parameters derived from a deep-sea sediment transect off southwest Africa reflect continental vegetation and climate conditions, Org. Geochem., 47, 109–119, 2012.